Title
Structural insight into transmissive mutant huntingtin species by correlative light and electron microscopy and cryo-electron tomography

Authors
Kuang, Xuyuan
Nunn, Kyle
Jiang, Jennifer
et al.

Publication Date
2021-06-30

DOI
10.1016/j.bbrc.2021.04.124

Peer reviewed

Biochemical and Biophysical Research Communications 560 (2021) 99–104

Contents lists available at ScienceDirect

Biochemical and Biophysical Research Communications

journal homepage: www.elsevier.com/locate/ybbrc

Structural insight into transmissive mutant huntingtin species by correlative light and electron microscopy and cryo-electron tomography

Xuyuan Kuang [a, b, c], Kyle Nunn [a, b], Jennifer Jiang [a, b], Paul Castellano [a, b], Uttara Hardikar [a, b], Arianna Horgan [b, d], Joyce Kong [b, e], Zhiqun Tan [f, g, **], Wei Dai [a, b, *]

[a] Department of Cell Biology and Neuroscience, Rutgers, The State University of New Jersey, Piscataway, NJ, 08854, USA
[b] Institute for Quantitative Biomedicine, Rutgers, The State University of New Jersey, Piscataway, NJ, 08854, USA
[c] Department of Hyperbaric Oxygen, Xiangya Hospital, Central South University, Changsha, Hunan, 410008, China
[d] School of Environmental and Biological Sciences, Rutgers, The State University of New Jersey, Piscataway, NJ, 08854, USA
[e] Ernest Mario School of Pharmacy, Rutgers, The State University of New Jersey, Piscataway, NJ, 08854, USA
[f] Department of Anatomy and Neurobiology, University of California Irvine School of Medicine, Irvine, CA, 29697, USA
[g] Institute for Memory Impairment and Neurological Disorders, University of California-Irvine, Irvine, CA, 29697, USA

ARTICLE INFO

Article history:
Received 27 April 2021
Accepted 29 April 2021
Available online 10 May 2021

Keywords:
Protein transmission
Mutant huntingtin
Extracellular vesicles
Cryo-electron tomography

ABSTRACT

Aggregates of mutant huntingtin (mHTT) containing an expanded polyglutamine (polyQ) tract are hallmarks of Huntington's Disease (HD). Studies have shown that mHTT can spread between cells, leading to the propagation of misfolded protein pathology. However, the structure of transmissive mHTT species, and the molecular mechanisms underlying their transmission remain unknown. Using correlative light and electron microscopy (CLEM) and cryo-electron tomography (cryo-ET), we identified two types of aggregation-prone granules in conditioned medium from PC12 cells expressing a mHTT N-terminal fragment: densities enclosed by extracellular vesicles (EVs), and uncoated, amorphous meshworks of heterogeneous oligomers that co-localize with clusters of EVs. *In vitro* assays confirmed that liposomes induce condensation of polyQ oligomers into higher-order assemblies, resembling the uncoated meshworks observed in PC12 conditioned medium. Our findings provide novel insights into formation and architecture of transmissive mHTT proteins, and highlight the potential role of EVs as both carriers and modulators of transmissive mHTT proteins.

1. Introduction

Huntington's disease (HD) is an inherited neurodegenerative disease that results in progressive motor, cognitive, and psychiatric impairment in patients. The disease is caused by an expansion of the polyglutamine (polyQ) tract within exon1 of the huntingtin (HTT) protein [1,2], leading to protein misfolding, accumulation of insoluble aggregates within cells and disturbance of normal cellular functions [3,4].

Recently, cell-to-cell transmission as an underlying mechanism for misfolded protein propagation and disease pathology has emerged as a central concept in neurodegenerative diseases, including HD [5], Alzheimer's [6] and Parkinson's diseases [7]. The presence of mutant huntingtin (mHTT) aggregates detected within intracerebral striatal tissue allografts in HD patients about 10 years post transplantation was one of the first demonstrations that misfolded protein transmission may challenge the clinical outcomes of cell replacement treatment strategies [8]. Further basic science and clinical research confirmed the presence of extracellular forms of mHTT proteins in biofluids or affected tissues [9–11]. Once internalized by recipient cells, mHTT proteins serve as seeds to nucleate intracellular aggregation (a process termed seeding), driving propagation of misfolded protein aggregation across cells and further aggravates disease progression [12–15]. However, the

* Corresponding author. Department of Cell Biology and Neuroscience, Rutgers, The State University of New Jersey, Piscataway, NJ, 08854, USA.
** Corresponding author. Department of Anatomy and Neurobiology, University of California Irvine School of Medicine, Irvine, CA, 29697, USA.
E-mail addresses: tanz@uci.edu (Z. Tan), wei.dai@rutgers.edu (W. Dai).

https://doi.org/10.1016/j.bbrc.2021.04.124
0006-291X/

structural and biochemical properties of misfolded mHTT as extracellular, transmissive entities are not well defined, limiting our understanding of their toxicity.

In this study, we used bioimaging tools of correlative light and electron microscopy (CLEM) and cryo-electron tomography (cryo-ET) to characterize the structures and seeding propensity of extracellular mHTT proteins present in the conditioned medium from a PC12 HD cell model. This work also revealed direct interactions between transmissive mHTT proteins and extracellular vesicles (EVs), implicating possible functional roles of EVs in modulating transmissive mHTT conformation and transmission between cells.

2. Materials and methods

2.1. Cell culture and preparation of conditioned medium

The 14A2.6 PC12 cell line was generated and cultured as described previously [16]. Following ponasterone A induction, these cells express truncated mHTT exon1 containing an expanded polyQ97 tract directly fused with an enhanced green fluorescence protein (EGFP) tag at the C-terminus (herein referred to as mHTTex1-EGFP). To generate conditioned medium for seeding assays and structural studies, 14A2.6 PC12 cells at 50% confluency were treated with 2.5 μM ponasterone A (Santa Cruz Biotechnologies) to induce expression of mHTTex1-EGFP. At 24 h post initiation of induction, the conditioned medium was collected and subjected to 10,000×*g* centrifugation (Beckman Coulter) for 10 min to remove cellular debris. The supernatant was collected and used for subsequent cell-based seeding assays, fluorescence microscopy, and CLEM and cryo-ET studies. As a control, growth medium from 14A2.6 PC12 cells cultured without ponasterone A was collected, and supplemented with 2.5 μM ponasterone A prior to use in seeding assays.

2.2. Immunodepletion of mHTTex1-EGFP by GFP trap

GFP-Trap®_A is an anti-GFP/EGFP antibody fragment conjugated to agarose beads that efficiently pull-downs GFP/EGFP-fusion proteins (Chromotek). The bead slurry was prepared following vendor instructions and added to the conditioned medium. The mixture was tumbled end-over-end at 4 °C for 1 h, and then centrifuged at 2,500×*g*, 4 °C for 2 min. The supernatant was collected and used in cell-based seeding assays. Agarose beads without conjugated antibodies were used as a control.

2.3. Cell-based seeding assay

To prepare cells for seeding assays, 14A2.6 PC12 cells in log phase growth were plated onto 0.01% poly-L-lysine (Millipore Sigma) treated 96-well black walled culture plates (CELLSTAR, Greiner) at approximately 50% confluency, and were induced with 1 μM ponasterone A for 24 h. At this induction condition, cells display basal levels of mHTTex1-EGFP expression and develop diffusive intracellular EGFP signals without visible puncta.

For quantification of seeding activities associated with transmissive mHTTex1-EGFP in the conditioned medium from induced 14A2.6 PC12 cells, freshly prepared conditioned medium, mHTTex1-EGFP depleted medium, and controls were added to cell assays. At 8 and 16 h post initiation of conditioned medium treatment, cells were washed in 37 °C PBS buffer (pH 7.0, Sigma-Aldrich), stained by Hoechst dye (Thermo Fisher Scientific) and then imaged in an IN Cell Analyzer 6000 (GE Healthcare) under a 20× objective at 9 fields per well. Quantification of cells with detectable bright puncta was done using the IN Cell Investigator Image Analysis Software (v. 1.6.3).

To quantify the seeding propensities for large mHTTex1-EGFP granules (uncoated assemblies and EV-enclosed mHTTex1-EGFP proteins) *vs* smaller aggregates, the conditioned medium was subjected to 100,000×*g* centrifugation for 2 h at 4 °C. The pellet was washed 3 times with PBS and resuspended in the same volume of fresh DMEM complete media supplemented with 2.5 μM ponasterone A. Growth medium from uninduced 14A2.6 PC12 cells was used as a negative control. Seeding activities associated with the large granules in the pellet fraction *vs.* the smaller species in the supernatant were assessed in the IN Cell Analyzer as described above.

2.4. Preparation of liposomes

Liposomes were prepared from porcine total brain extract following a standard liposome formulation protocol (Avanti Polar Lipids Inc.). The liposome solutions were extruded 10 times through a mini-extruder on a heating block at 60 °C through two layers of polycarbonate filters and generated liposomes of 100–500 nm in size, similar to the EV size distribution observed in the conditioned medium.

2.5. In vitro liposome - polyQ binding assay

PolyQ40 seeds were prepared from synthetic polyQ40 peptides as described previously [11]. For liposome-polyQ binding assay, polyQ40 oligomers were mixed with freshly-made liposomes at the final polyQ40 concentration of 2 μM, and incubated at room temperature for 8 h. An aliquot of the liposome-polyQ sample was then collected and prepared for tomography studies. For controls, polyQ40 oligomers were diluted to the final concentration of 2 μM or 5 μM, incubated at room temperature for 8 h, and prepared for imaging by cryo-ET.

2.6. Grid preparation

The conditioned medium, polyQ40 oligomers, or liposome-polyQ samples were first mixed with 10 nm gold fiducials (EMS) to facilitate tilt series alignment during data processing. An aliquot of 3.5 μl of sample was applied to glow-discharged Quantifoil grids (for polyQ40 oligomers and liposome-polyQ samples) or Quantifoil finder grids (for conditioned medium) and then plunge frozen using a Leica EM GP plunger (Leica Microsystems).

2.7. Correlative light and electron microscopy

Conditioned medium grids were loaded into a Leica DM6 FS microscope equipped with a 50× objective and a DFC 365 FX camera. Fluorescence and corresponding bright field montage images of the grids were acquired using the Leica LASX software. Areas of the grid with $EGFP^+$ densities were marked as targets.

2.8. Cryo-ET data collection and data processing

Conditioned medium grids that were pre-screened on the Leica CLEM were loaded into a Talos Arctica microscope (Thermo Fisher Scientific) equipped with a post-column BioQuantum energy filter and K2 direct electron detector (Gatan, Inc.). A low-magnification (900x) montage of the entire grid was collected and manually aligned to the fluorescence image of the same grid to identify $EGFP^+$ mHTT aggregates. 2D projection images and tilt series of target areas were collected at 31,000× magnification for EV-enclosed mHTTex1-EGFP densities with a pixel size of 4.30 Å/pixel. Uncoated mHTTex1-EGFP assemblies were imaged at

39,000× magnification with a corresponding pixel size of 3.49 Å/pixel. Imaging settings used were spot size 8, 100 μm condenser aperture, 100 μm objective aperture, 20 eV energy filter slit, and −5 μm defocus. Typically, a tilt series ranges from −60° to 60° at 3° step increments. The total dose is ~80–100 e/Å^2 per tilt series.

Tilt series for polyQ40 oligomers and liposome-polyQ samples were collected at 31,000x or 39,000× magnification, respectively, using the same imaging configurations.

Tilt series alignment and reconstruction were done in IMOD [17]. 3D map visualization and annotation were done using UCSF Chimera (University of California, San Francisco) [18].

3. Results

3.1. Conditioned medium from 14A2.6 PC12 cells contains extracellular, seeding-competent transmissive mHTT proteins

To investigate the structural and biochemical properties of transmissive mHTT species, we used conditioned medium from 14A2.6 PC12 cells as a model system [11,16]. Following ponasterone A induction, these cells express truncated mHTT exon1 containing an expanded polyQ tract directly fused with an EGFP tag at the C-terminus (mHTTex1-EGFP). At 24 h post-induction, aggregates were observed in the cytoplasm, progressing from diffuse proteins to small aggregates, and then to micron-sized inclusions as indicated by bright EGFP signals. Concurrent with the formation of intracellular inclusions, microscopic granules of mHTTex1-EGFP proteins also developed in the extracellular space (Fig. 1a). A control PC12 cell line that expresses EGFP-labeled truncated wild type HTT exon1 containing a polyQ25 tract showed no detectable intracellular or extracellular bright puncta under the same experimental conditions (Fig. 1b), indicating that the extended polyQ tract in mHTT proteins, not the EGFP tag, causes the formation of intracellular inclusions and extracellular granules.

To characterize the level of extracellular mHTT proteins in the conditioned medium from induced 14A2.6 cells, we measured the seeding propensity of the conditioned medium in a cell-based seeding assay using cells exhibiting basal expression of mHTT proteins [11]. Conditioned medium collected 24 h post-induction efficiently promoted inclusion formation in cells at 8 and 16 h following treatment with the conditioned medium. This observation confirmed that the conditioned medium contains seeding-competent entities. The seeding efficiency was significantly attenuated when mHTTex1-EGFP proteins were depleted by GFP-trap (Fig. 1c), indicating that extracellular mHTTex1-EGFP is indeed responsible for the seeding propensity of the conditioned medium.

3.2. CLEM and cryo-ET resolved the 3D architecture of two types of transmissive mHTT granules

We observed two types of microscopic mHTTex1-EGFP species present in the conditioned medium from induced 14A2.6 PC12 cells: bright puncta with clear boundaries, and dim granules of various sizes without defined edges (Fig. 2a). With extended induction of mHTTex1-EGFP expression, the number of the bright puncta steadily increases, but the abundance of the diffuse granules does not correlate with the intracellular mHTT level, suggesting they represent more dynamic entities. To investigate structural identity of the granules, we first applied CLEM to identify EGFP$^+$ species, and then imaged by cryo-ET to resolve their structures. Tomograms revealed that the bright puncta are extracellular vesicles (EVs) enclosing oligomeric mHTTex1-EGFP densities (Fig. 2b–d, Supplementary Video 1), while the dim granules correspond to uncoated meshworks of densities that are consistent in appearance with assemblies of mHTT oligomers (Fig. 2e–g, Supplementary Video 2). Studies on mHTT secretion mechanisms have revealed that mHTT proteins can exit cells *via* an unconventional late endosomal and lysosomal secretory pathway in a free, non-vesicular form [19,20], or through an exosome or microvesicle-mediated transport in an extracellular vesicle-enclosed form [10,21]. The two types of granules likely represent transmissive mHTT released through different mechanisms.

Supplementary video related to this article can be found at https://doi.org/10.1016/j.bbrc.2021.04.124

We also observed that clusters of EVs surround the uncoated mHTTex1-GFP (Fig. 2f and g). Sizes of these EVs ranged from hundreds of nanometers to several micrometers, suggesting that they could be microvesicles, apoptotic bodies, or exosomes. In tomograms of dim granules, EVs typically exhibited some levels of deformation and changes in membrane curvature, which may be attributed to interactions with the uncoated mHTT meshwork. In the growth medium from uninduced 14A2.6 PC12 cells, we observed EVs of a similar size range with a more spherical morphology (Fig. 2h), supporting this notion.

To further examine the association between EVs and extracellular mHTT species, the conditioned medium from induced PC12 cells was stained by Nile Red to detect EVs, and then subjected to fluorescence microscopy. The colocalization pattern of EGFP and Nile Red signals confirms that many large mHTTex1-EGFP granules are either enclosed by EVs, or exist as assemblies associated

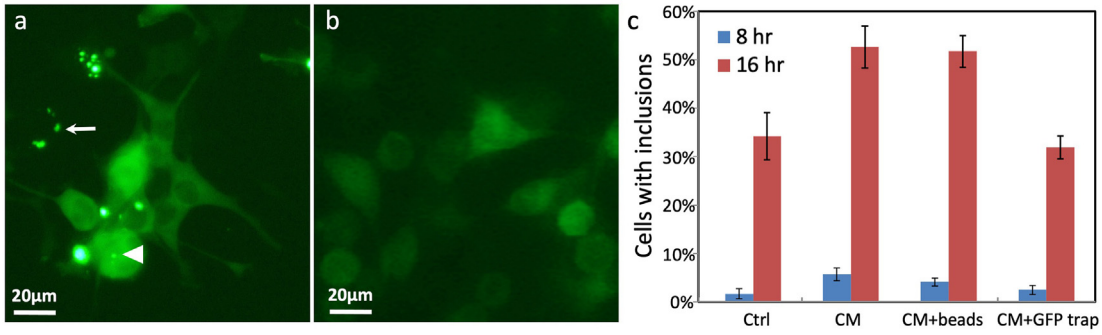

Fig. 1. Conditioned medium from induced 14A2.6 PC12 cells contains seeding-competent mHTT species. (a) A fluorescence image of induced 14A2.6 PC12 cells showing intracellular puncta (arrowhead) and extracellular granules (arrow) of mHTTex1-EGFP. **(b)** A fluorescence image of control 14A2.6 PC12 cells. **(c)** Conditioned medium from induced 14A2.6 PC12 cells demonstrates mHTTex1-EGFP dependent seeding propensity in cell-based seeding assays [T-test, N = 6, p values: 0.034 (8 h), 0.018 (16 h)]. Cells were treated with: Ctrl: growth medium collected from uninduced PC12 cells supplemented with 2.5 μM ponasterone A. CM: conditioned medium from 14A2.6 PC12 cells after 24 h of 2.5 μM ponasterone A induction. CM + beads: conditioned medium that is mixed with agarose beads only. CM + GFP-trap: conditioned medium with mHTTex1-EGFP depleted by agarose beads conjugated with an anti-GFP/EGFP antibody fragment.

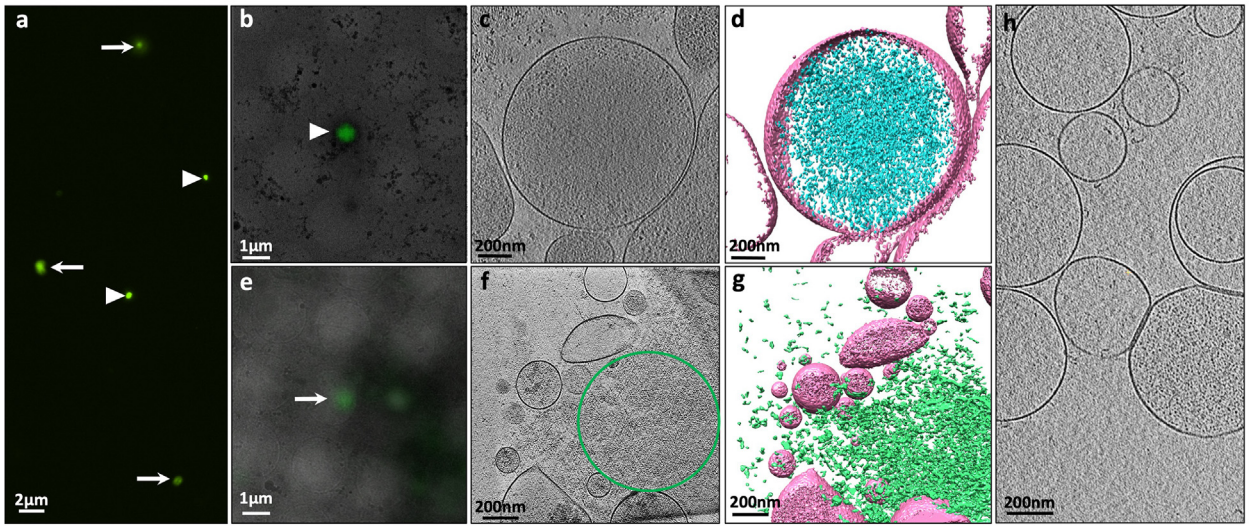

Fig. 2. 3D structure of transmissive mHTT granules revealed by CLEM and cryo-ET. **(a)** A fluorescent light microscopy image of the two types of mHTTex1-EGFP granules in the conditioned medium from induced 14A2.6 PC12 cells. Arrowhead: bright, dense puncta; Arrow: dim granules without clear edges. **(b)** Correlative light microscopy and low magnification electron microscopy (EM) images of a representative bright punctum (arrowhead). **(c)** Slice view of a tomogram of the mHTTex1-EGFP punctum in (b). **(d)** Isosurface view of the tomogram showing an EV enclosing mHTTex1-EGFP densities (Pink: EV membrane; Teal: vesicle-enclosed mHTTex1-EGFP densities). **(e)** Correlative light microscopy and low magnification EM images of a representative diffuse granule (arrow). **(f)** Slice view of the tomogram taken at the $EGFP^+$ region. Green circle: location of $EGFP^+$ density as shown in (e). **(g)** 3D isosurface view of the tomogram of uncoated mHTTex1-EGFP meshwork (Pink: EVs; Green: uncoated mHTTex1-EGFP densities). **(h)** Slice view of a tomogram of EVs in the growth medium from control, uninduced 14A2.6 PC12 cells.

externally on EV membrane surfaces (Fig. 3a). This finding is consistent with observations from cryo-ET studies and demonstrates potential roles of EVs in mHTT transmission.

The $EGFP^+$ granules represent extracellular mHTT species secreted by induced cells or released following cell membrane rupture. To analyze the seeding efficiency of these large granules (EV-enclosed or EV membrane-associated) *vs* smaller, freestanding oligomers or protofibrils undetectable by fluorescence microscopy, we separated the two fractions by ultracentrifugation. In cell-based seeding assays, 53% of cells treated with the resuspended pellet fraction containing EV-associated granules developed mHTT inclusions following a 24-h treatment. On the other hand, 31% of cells treated with the supernatant fraction containing small oligomers or protofibrils developed inclusions (Fig. 3b). This difference in inclusion formation suggests that the mHTT granules in the conditioned medium have overall higher seeding capacity compared to the smaller, freestanding species in the supernatant. These extracellular granules represent the primary seeding effectors in the conditioned medium.

3.3. Liposomes modulate condensation of polyQ proteins into higher-order assemblies

The observation that the uncoated extracellular mHTTex1-EGFP species exist in the conditioned medium as higher-order assemblies is unexpected. The concentration of mHTT proteins in the conditioned medium is in the low nanomolar range [11], which is usually too low for mHTT proteins to spontaneously aggregate into large assemblies. Co-localization of EVs and the uncoated assemblies of mHTTex1-EGFP proteins led to the postulation that EVs may modulate mHTT protein conformation and promote the formation of the uncoated transmissive mHTT assemblies observed in the conditioned medium.

To test this hypothesis, we developed an *in vitro* reconstituted system consisting of preformed liposomes and synthetic polyQ peptides. In mHTT proteins, the polyQ tract is responsible for their

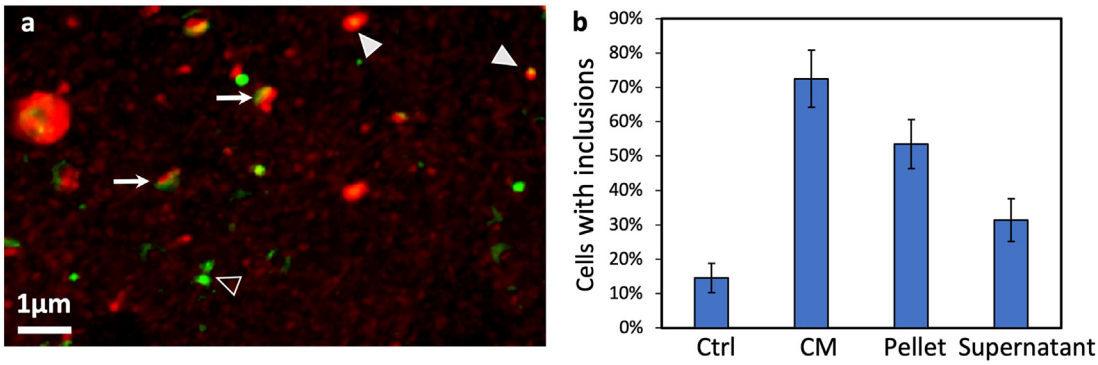

Fig. 3. Microscopic mHTTex1-EGFP granules in the conditioned medium from induced 14A2.6 PC12 cells are effective seeds. **(a)** A fluorescence confocal image showing association of mHTTex1-EGFP granules with Nile Red-stained EVs (externally: arrows; internally: solid arrowheads). Aggregates of mHTTex1-EGFP that are not directly engaged in interactions with EVs are labeled by a hollow arrowhead. **(b)** Seeding efficiency of mHTTex1-EGFP granules in the 100,000 g centrifugation pellet and smaller mHTTex1-EGFP species in the supernatant. Ctrl: control growth medium collected from uninduced 14A2.6 PC12 cells supplemented with 2.5 μM ponasterone A; CM: conditioned medium from 14A2.6 PC12 cells after 2.5 μM ponasterone A induction for 24 h; Pellet: pellet fraction obtained from the 100,000 g centrifugation that was resuspended in an equal volume of fresh medium containing 2.5 μM ponasterone A; Supernatant: supernatant obtained from the 100,000 g centrifugation.

aggregation behaviors [22,23]. In the reconstituted system, we used a polyQ peptide of 40 glutamines (polyQ40) as a simplified model of mHTT exon 1. This system is also free of small molecules and other soluble effectors that are present in the conditioned medium and would otherwise complicate the analysis.

Cryo-ET of the polyQ40 peptide alone revealed oligomers that are extremely heterogeneous, ranging from annular ring/disc structures to elongated densities (Fig. 4a and b, Supplementary Video 3). Increasing the concentration of polyQ40 peptides from 2 μM to 5 μM led to an increase in the distribution of oligomers in the tomograms and a higher abundance of larger oligomers (Fig. 4b). At both concentrations, polyQ40 peptides are present as disperse, polymorphic densities, supporting the notion that the mHTT aggregation pathway features a heterogeneous population of distinct oligomers as intermediate species [24].

Supplementary video related to this article can be found at https://doi.org/10.1016/j.bbrc.2021.04.124

Addition of liposomes to the polyQ40 peptides induced condensation of polyQ40 oligomers into higher-order assemblies (Fig. 4c and d, Supplementary Video 4) that resembled the uncoated mHTTex1-EGFP meshworks observed in the conditioned medium from 14A2.6 PC12 cells. These assemblies directly engage with liposome surfaces, causing membrane deformation, changes in curvature, and disruption of membrane integrity. These findings corroborate previous observations with EVs found near mHTTex1-EGFP densities in the conditioned medium (Fig. 2g). Our results suggest that interactions with EVs may have induced the formation of the uncoated transmissive mHTT assemblies in the conditioned medium. This modulation is polyQ-dependent, since the polyQ40 peptides used in this *in vitro* system lacked both the N17 and proline-rich flanking regions in mHTT exon1.

Supplementary video related to this article can be found at https://doi.org/10.1016/j.bbrc.2021.04.124

4. Discussion

By combining CLEM and cryo-ET, we have resolved transmissive mHTT proteins in the conditioned medium from 14A2.6 PC12 cells as EV-enclosed, oligomeric densities, or as uncoated amorphous meshworks that are externally associated with EV membranes. The polymorphic, amorphous nature of transmissive mHTT species is likely linked to the intrinsically disordered property of the polyQ tract [25,26], and is structurally distinct from fibrillar aggregates that are often used in *in vitro* seeding assays [27]. Numerous experiments have shown that biologically-derived samples, cerebrospinal fluid (CSF) from HD patients or growth medium from HD cell models, have dramatically higher seeding efficiencies compared to synthetic seeds [11,28]. The differential seeding efficiency between transmissive species in biologically-derived samples and pure, synthetic polyQ seeds, therefore, can be attributed to different mHTT conformations, or the modulatory effects of endogenous cofactors, such as EVs, that are present in biologically-derived samples.

Previous studies on mHTT protein transmission suggested that mHTT can be secreted to the extracellular space as vesicle-enclosed or free-standing forms [10,19–21]. The observation of uncoated mHTT granules in the conditioned medium of induced 14A2.6 PC12 cells is consistent with previous findings that mHTT components in the cerebrospinal fluid were directly detected and depleted by antibodies targeting expanded polyQ tracts [11,28]. The presence of EVs enclosing mHTT proteins suggests that EVs are actively involved in misfolded protein propagation by transporting

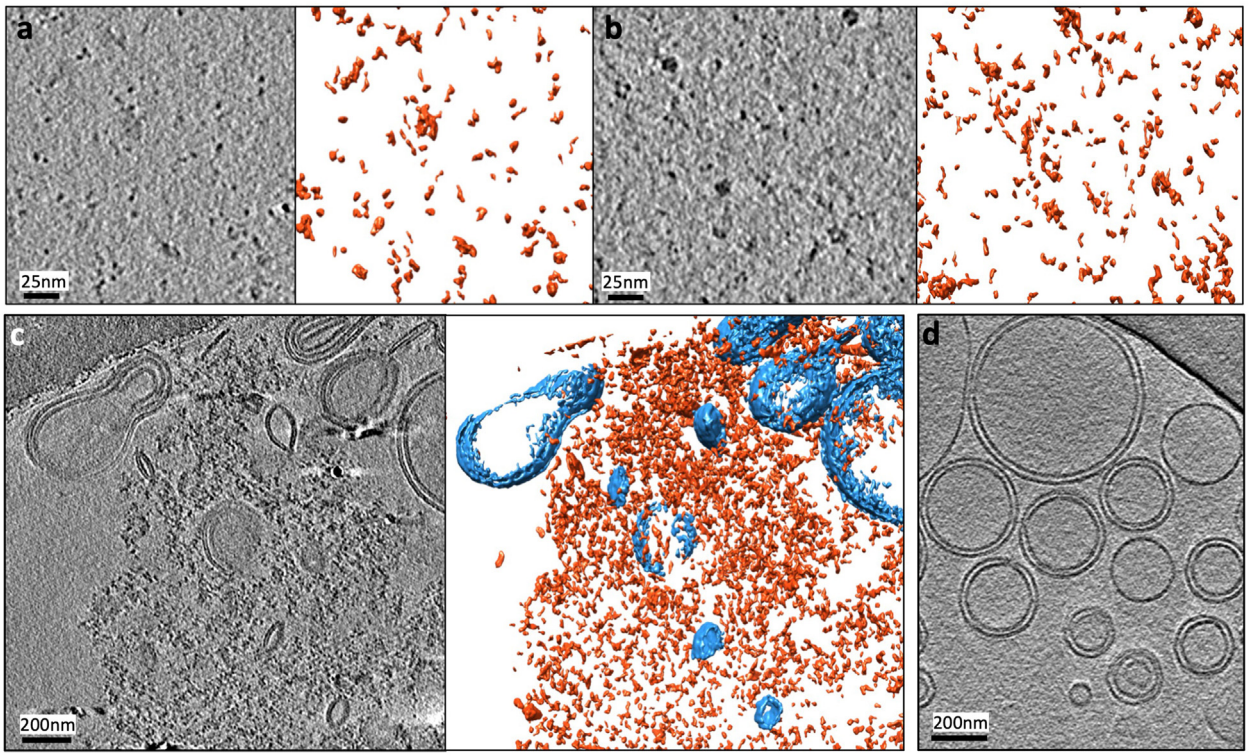

Fig. 4. Liposome-polyQ interactions induce formation of assemblies of polyQ40 peptides. **(a)** Slice (left) and isosurface (right) views of a tomogram showing polyQ40 oligomers at 2 μM polyQ40 concentration. **(b)** Slice (left) and isosurface (right) views of a tomogram of polyQ40 oligomers at 5 μM polyQ40 concentration. **(c)** Slice (left) and isosurface (right) views of a tomogram of 2 μM polyQ40 oligomers and preformed liposomes. (Blue: liposomes; Orange: polyQ40 oligomers). **(d)** Slice view of a tomogram of preformed liposomes alone.

molecular cargoes between cells [15,29–32]. Additionally, the association of uncoated mHTT meshworks on EV membrane surfaces and results from the *in vitro* experiment suggest that EV membranes are capable of inducing condensation of mHTT proteins into large assemblies. Taken together, these findings suggest novel roles of EVs in mHTT transmission: they may function as both biological couriers between cells, and as modulators of transmissive mHTT protein conformations and higher-order assembling. Further elucidation of the molecular mechanisms underpinning mHTT transmission represents a critical step in understanding HD pathology, and in developing new strategies that ameliorate disease progression by slowing down misfolded protein transmission.

Data availability statement

Tomograms of EV-enclosed and uncoated meshwork of mHTTex1-EGFP densities from the conditioned medium of induced 14A2.6 PC12 cells, 2 μM polyQ40 oligomers, and liposome-polyQ sample have been deposited in the EMDataBank under accession codes EMD-23756, EMD-23768, EMD-23737 and EMD-23762 respectively.

Declaration of competing interest

The authors declare that they have no known competing financial interests or personal relationships that could have appeared to influence the work reported in this paper.

Acknowledgements

This work was supported by the National Science Foundation [grant number MCB-2046180]; Rutgers Busch Biomedical Research Grant to W.D.; X. K. was partially supported by the Chinese Scholarship Council (award number 201606375128). Z. T. acknowledges his support from the National Institute of Health [grant number P01 NS092525]. CLEM and cryo-ET data was collected at Rutgers CryoEM & Nanoimaging Facility. We thank Jason Kaelber and Emre Firlar for their support in data collection. We thank Zhiyong Bai for collecting the tilt series of 2 μM polyQ40 oligomers and Charles Glabe for providing the polyQ40 peptide.

References

[1] M.E. MacDonald, C.M. Ambrose, M.P. Duyao, et al., A novel gene containing a trinucleotide repeat that is expanded and unstable on Huntington's disease chromosomes. The Huntington's Disease Collaborative Research Group, Cell 72 (1993) 971–983.
[2] C.A. Ross, E.H. Aylward, E.J. Wild, et al., Huntington disease: natural history, biomarkers and prospects for therapeutics, Nat. Rev. Neurol. 10 (2014) 204–216, https://doi.org/10.1038/nrneurol.2014.24.
[3] F.J.B. Bäuerlein, I. Saha, A. Mishra, et al., In situ architecture and cellular interactions of PolyQ inclusions, Cell 171 (2017) 1–9, https://doi.org/10.1016/j.cell.2017.08.009.
[4] J.Y. Chen, M. Parekh, H. Seliman, et al., Heat shock promotes inclusion body formation of mutant huntingtin (mHtt) and alleviates mHtt-induced transcription factor dysfunction, J. Biol. Chem. 293 (2018) 15581–15593, https://doi.org/10.1074/jbc.RA118.002933.
[5] M. Masnata, F. Cicchetti, The evidence for the spread and seeding capacities of the mutant huntingtin protein in in vitro systems and their therapeutic implications, Front. Neurosci. 11 (2017) 647, https://doi.org/10.3389/fnins.2017.00647.
[6] N.V. Mohamed, T. Herrou, V. Plouffe, et al., Spreading of tau pathology in Alzheimer's disease by cell-to-cell transmission, Eur. J. Neurosci. 37 (2013) 1939–1948, https://doi.org/10.1111/ejn.12229.
[7] J.Y. Li, E. Englund, J.L. Holton, et al., Lewy bodies in grafted neurons in subjects with Parkinson's disease suggest host-to-graft disease propagation, Nat. Med. 14 (2008) 501–503, https://doi.org/10.1038/nm1746.
[8] F. Cicchetti, S. Lacroix, G. Cisbani, et al., Mutant huntingtin is present in neuronal grafts in huntington disease patients, Ann. Neurol. (2014), https://doi.org/10.1002/ana.24174.
[9] I. Melentijevic, M.L. Toth, M.L. Arnold, et al., C. elegans neurons jettison protein aggregates and mitochondria under neurotoxic stress, Nature (2017), https://doi.org/10.1038/nature21362.
[10] I. Jeon, F. Cicchetti, G. Cisbani, et al., Human-to-mouse prion-like propagation of mutant huntingtin protein, Acta Neuropathol. 132 (2016) 577–592, https://doi.org/10.1007/s00401-016-1582-9.
[11] Z. Tan, W. Dai, T.G. van Erp, et al., Huntington's disease cerebrospinal fluid seeds aggregation of mutant huntingtin, Mol. Psychiatr. 20 (2015) 1286–1293, https://doi.org/10.1038/mp.2015.81.
[12] P.H. Ren, J.E. Lauckner, I. Kachirskaia, et al., Cytoplasmic penetration and persistent infection of mammalian cells by polyglutamine aggregates, Nat. Cell Biol. 11 (2009) 219–225, https://doi.org/10.1038/ncb1830.
[13] F. Cicchetti, S. Saporta, R.A. Hauser, et al., Neural transplants in patients with Huntington's disease undergo disease-like neuronal degeneration, Proc. Natl. Acad. Sci. U. S. A. 106 (2009) 12483–12488, https://doi.org/10.1073/pnas.0904239106.
[14] A.H. Jansen, K.L. Batenburg, E. Pecho-Vrieseling, et al., Visualization of prion-like transfer in Huntington's disease models, Biochim. Biophys. Acta 1863 (2017) 793–800, https://doi.org/10.1016/j.bbadis.2016.12.015.
[15] X. Zhang, E.R. Abels, J.S. Redzic, et al., Potential transfer of polyglutamine and CAG-repeat RNA in extracellular vesicles in huntington's disease: background and evaluation in cell culture, Cell. Mol. Neurobiol. 36 (2016) 459–470, https://doi.org/10.1007/s10571-016-0350-7.
[16] B.L. Apostol, A. Kazantsev, S. Raffioni, et al., A cell-based assay for aggregation inhibitors as therapeutics of polyglutamine-repeat disease and validation in Drosophila, Proc. Natl. Acad. Sci. U. S. A. 100 (2003) 5950–5955, https://doi.org/10.1073/pnas.2628045100.
[17] D.N. Mastronarde, S.R. Held, Automated tilt series alignment and tomographic reconstruction in IMOD, J. Struct. Biol. (2016), https://doi.org/10.1016/j.jsb.2016.07.011.
[18] E.F. Pettersen, T.D. Goddard, C.C. Huang, et al., UCSF Chimera - a visualization system for exploratory research and analysis, J. Comput. Chem. 25 (2004) 1605–1612.
[19] K. Trajkovic, H. Jeong, D. Krainc, Mutant huntingtin is secreted via a late endosomal/lysosomal unconventional secretory pathway, J. Neurosci. 37 (2017) 9000–9012, https://doi.org/10.1523/JNEUROSCI.0118-17.2017.
[20] K. Trajkovic, H. Jeong, D. Krainc, Mutant huntingtin secretion in Neuro2A cells and rat primary cortical neurons, Bio Protoc 8 (2018) e2675, https://doi.org/10.21769/BioProtoc.2675.
[21] E. Pecho-Vrieseling, C. Rieker, S. Fuchs, et al., Transneuronal propagation of mutant huntingtin contributes to non-cell autonomous pathology in neurons, Nat. Neurosci. 17 (2014) 1064–1072, https://doi.org/10.1038/nn.3761.
[22] A. Gruber, D. Hornburg, M. Antonin, et al., Molecular and structural architecture of polyQ aggregates in yeast, Proc. Natl. Acad. Sci. U. S. A. 115 (2018) E3446–E3453, https://doi.org/10.1073/pnas.1717978115.
[23] T. Yushchenko, E. Deuerling, K. Hauser, Insights into the aggregation mechanism of PolyQ proteins with different glutamine repeat lengths, Biophys. J. 114 (2018) 1847–1857, https://doi.org/10.1016/j.bpj.2018.02.037.
[24] J. Legleiter, E. Mitchell, G.P. Lotz, et al., Mutant huntingtin fragments form oligomers in a polyglutamine length-dependent manner in vitro and in vivo, J. Biol. Chem. 285 (2010) 14777–14790, https://doi.org/10.1074/jbc.M109.093708.
[25] P. Mier, L. Paladin, S. Tamana, et al., Disentangling the complexity of low complexity proteins, Briefings Bioinf. 21 (2020) 458–472, https://doi.org/10.1093/bib/bbz007.
[26] A. Toto, F. Malagrino, L. Visconti, et al., Templated folding of intrinsically disordered proteins, J. Biol. Chem. 295 (2020) 6586–6593, https://doi.org/10.1074/jbc.REV120.012413.
[27] S. Gupta, S. Jie, D.W. Colby, Protein misfolding detected early in pathogenesis of transgenic mouse model of Huntington disease using amyloid seeding assay, J. Biol. Chem. 287 (2012) 9982–9989, https://doi.org/10.1074/jbc.M111.305417.
[28] E.J. Wild, R. Boggio, D. Langbehn, et al., Quantification of mutant huntingtin protein in cerebrospinal fluid from Huntington's disease patients, J. Clin. Invest. 125 (2015) 1979–1986, https://doi.org/10.1172/JCI80743.
[29] C. Quek, A.F. Hill, The role of extracellular vesicles in neurodegenerative diseases, Biochem. Biophys. Res. Commun. 483 (2017) 1178–1186, https://doi.org/10.1016/j.bbrc.2016.09.090.
[30] S. Liu, A. Hossinger, S. Gobbels, et al., Prions on the run: how extracellular vesicles serve as delivery vehicles for self-templating protein aggregates, Prion 11 (2017) 98–112, https://doi.org/10.1080/19336896.2017.1306162.
[31] M.C. Didiot, L.M. Hall, A.H. Coles, et al., Exosome-mediated delivery of hydrophobically modified siRNA for huntingtin mRNA silencing, Mol. Ther. 24 (2016) 1836–1847, https://doi.org/10.1038/mt.2016.126.
[32] B.L. Tang, Unconventional secretion and intercellular transfer of mutant huntingtin, Cells 7 (2018), https://doi.org/10.3390/cells7060059.